





# Surface-Engineered Super-Paramagnetic Iron Oxide Nanoparticles For Chromium Removal

This article was published in the following Dove Press journal:  
*International Journal of Nanomedicine*

Antony V Samrot <sup>1</sup>  
Chamarthy Sai Sahithya <sup>2</sup>  
Jenifer Selvarani A <sup>2</sup>  
Senthilkumar Pachiyappan <sup>3</sup>  
Suresh Kumar S<sup>4,5</sup>

<sup>1</sup>Department of Biomedical Sciences, Faculty of Medicine and Biomedical Sciences, MAHSA University, Jenjarom, Selangor 42610, Malaysia; <sup>2</sup>Department of Biotechnology, School of Bio and Chemical Engineering, Sathyabama Institute of Science and Technology, Chennai, Tamil Nadu 600119, India; <sup>3</sup>Department of Chemical Engineering, School of Bio and Chemical Engineering, Sathyabama Institute of Science and Technology, Chennai, Tamil Nadu 600119, India; <sup>4</sup>Department of Medical Microbiology and Parasitology, Faculty of Medicine and Health Sciences, Universiti Putra Malaysia (UPM), Serdang, Selangor 43400, Malaysia; <sup>5</sup>Genetics and Regenerative Medicine Research Centre, Faculty of Medicine and Health Sciences, Universiti Putra Malaysia (UPM), Serdang, Selangor 43400, Malaysia

**Background:** Super-paramagnetic iron oxide nanoparticles (SPIONs) are widely used metal nanoparticles for various applications for its magnetic property and biocompatibility. In recent years, pollution of our environment especially with heavy metals in waterbodies has become a major threat and has left us very minimal sources of freshwater to drink. SPIONs or surface modified SPIONs can be used to remove these heavy metals

**Methods:** SPIONs were synthesized by co-precipitation method and further coated with a biopolymer, chitosan. Chromium solution was treated with the synthesized SPIONs to study the efficiency of chromium removal by surface adsorption. Later, the adsorption was analysed by direct and indirect analysis methods using UV-VIS spectrophotometry and isotherm studies.

**Results:** Stable chitosan-coated SPIONs were synthesized and they adsorbed chromium better than the uncoated SPIONs, where it was adsorbing up to 100 ppm. Adsorption was found to be increasing with decrease in pH.

**Conclusion:** The surface-modified SPIONs expressed cumulative adsorption action. Even after the adsorption studies, chitosan-coated SPIONs were possessing magnetic property. Thus, the surface-modified SPIONs can become an ideal nanotechnology tool to remove the chromium from groundwater.

**Keywords:** SPIONs, chitosan coating, chromium, adsorption, isotherm studies

## Introduction

The industrialization and exploitation of earth have led to an increase in pollution of resources at an alarming rate. One of the most concerned areas of these effects is water. Water pollution is increasing day by day due to contamination of heavy metal ions, toxins, dyes, waste, etc. The main reason for this pollution is due to the release of unprocessed and untreated effluents of tanneries, electronic industries, etc. Among the causes, heavy metal contamination is very dangerous and poses an unfaltering risk to all the living communities. The elements which have a specific density more than 5 g/cm<sup>3</sup> can be generally termed as heavy metals. A lot of these heavy metal ions are present in the environment naturally and also in human bodies as micronutrients, but heavy metals such as mercury, lead, chromium, arsenic are extremely toxic and hazardous to the environment when accumulated. It leads to biomagnification which results in the accumulation of heavy metals in body organs, thus leading to organ failure, genotoxicity and carcinogenicity.<sup>1,2</sup> Chromium (Cr) is a heavy metal with an atomic number 24 and atomic weight 51.996, which is present in different oxidation states such as chromium, trivalent chromium (Cr<sup>3+</sup>) and hexavalent chromium (Cr<sup>6+</sup>). Among them, hexavalent chromium is said to be highly toxic since it can pass through cell wall causing noxious influence inside

Correspondence: Antony V Samrot  
Department of Biomedical Sciences,  
Faculty of Medicine and Biomedical  
Sciences, MAHSA University, Jenjarom,  
Selangor 42610, Malaysia  
Email antonyasamrot@gmail.com

Suresh Kumar Subbiah  
Department of Medical Microbiology and  
Parasitology, Faculty of Medicine and  
Health Sciences, Universiti Putra Malaysia  
(UPM), Serdang, Selangor 43400, Malaysia  
Email sureshkudsc@gmail.com

cells and also causes cancers. Hexavalent chromium is a common pollutant seen in natural waters due to the industrial wastewater effluent, especially, tanning and leather industries. Generally, the maximum allowed limit of chromium in groundwater is 0.05 ppm.<sup>3</sup> Short-term exposure of chromium levels above the maximum contaminant level causes skin and stomach irritation.<sup>4,5</sup> Long-term exposure can cause dermatitis, damage to liver, nerve tissue damage, and also death.<sup>6,7</sup> Hence, removing these hazardous pollutants is being prioritized and researched to possibly reduce pollution. Nanotechnology can pave the way for removing these pollutants from water.

Nanotechnology can be defined as a branch of science that deals with particles that fall in the size range of 1–100 nm.<sup>8</sup> Nanotechnology and the study of nanosized objects require knowledge on diverse fields of science such as surface chemistry,<sup>9</sup> molecular engineering, semiconductor physics, biology, and photoreduction of heavy metals<sup>10–14</sup> etc. and are a convergence of such different traditional sciences.<sup>15</sup> Their small size and better properties such as surface to volume ratio, surface interaction and surface energy when compared to their bulk material are one of the reasons why nanotechnology has been one of the rapidly growing fields of science.<sup>16</sup>

Iron oxide nanoparticles have attracted a lot of interest in the scientific and research community due to its unique properties such as small size, superparamagnetic nature, surface charge, full spin polarization, and high curie temperature.<sup>17</sup> Individual SPIONs have a large magnetic moment within them and thus enabling those to behave as giant paramagnetic atom and respond to the applied magnetic field and lose their magnetism once the external magnetic field is removed.<sup>18</sup> Super-paramagnetic iron oxide nanoparticles (SPIONs) include magnetite ( $\text{Fe}_3\text{O}_4$ ), maghemite ( $\gamma\text{-Fe}_2\text{O}_3$ ), hematite ( $\alpha\text{-Fe}_2\text{O}_3$ ), and other ferrites.<sup>19</sup> These features and properties of iron oxide nanoparticles have enabled them to be utilized in a lot of applications such as targeted drug delivery,<sup>20</sup> hyperthermia,<sup>21,22</sup> imaging,<sup>23,24</sup> tissue engineering,<sup>25</sup> stem cell labelling,<sup>26</sup> in-vitro-bio-separation, and heavy metal removal.<sup>27</sup> Although used in diverse ways, the major challenge faced when working with SPIONs is to make them monodispersed which is possible by surface engineering or surface modification by a functionalizing agent or a potent biopolymer.

One of the best biopolymers to coat onto SPIONs to increase the stability as well as the adsorption efficiency for a cumulative effect is chitosan. Chitosan has widely

been studied as a pollutant adsorption from aqueous solutions due to its cationic character. The presence of reactive functional groups such as amino and hydroxyl groups in polymer chains of chitosan act as the active sites for adsorption in addition to its low cost and local availability, high reactivity, excellent chelation behaviour, and high selectivity towards chromium heavy metals.<sup>28–30</sup>

The rate and nature of adsorption are usually analysed and studied using adsorption isotherms. It explains the amount of adsorbate adsorbed on the adsorbent as a function of its pressure (if gas) or concentration (for liquid phase solutes) at constant temperature. The basic adsorption isotherms used to study the adsorption process are Langmuir isotherm, Freundlich isotherm, and Temkin isotherm. In this study, SPIONs were coated with chitosan and used as adsorbate to remove chromium from water and subjected for isotherm studies.

## Materials And Methods

### Materials

The materials used in this study are all of analytical grade. The chemicals used are ferric chloride (Loba Chemie), ferrous chloride (Loba Chemie), sodium hydroxide (SRL), ammonium solution (SRL), hydrochloric acid, chitosan (SRL), acetic acid (RANKEM), ethanol, sulfuric acid, nitric acid, diphenyl carbazide, potassium dichromate, and methanol. The whole study was done using nitrogen purged MilliQ water.

### Methods

#### Synthesis Of Super-Paramagnetic Iron Oxide Nanoparticles (SPIONs)

All the chemicals used for SPIONs production were prepared in nitrogen purged MilliQ water. SPIONs were synthesized using 1M of  $\text{FeCl}_3$  and 3M of  $\text{FeCl}_2$  which were prepared separately. Equal volumes (25 mL) of the above precursors were brought into a mixture and stirred well. While heating the prepared precursor iron mixture at 60 °C, 50 mL of 8M NaOH was added in drops on constant vigorous stirring with simultaneous dropwise addition of ammonia solution until a black precipitate is formed. The alkali pH of the precipitate solution was brought down to neutral by adding 1N HCl. Thus, formed black particles were allowed to settle and separate out from the mixture by applying a magnetic field. The collected particles were washed repeatedly using nitrogen purged MilliQ water until neutral pH and then freeze-dried to remove moisture.

### Preparation Of Chitosan-Coated SPIONs (Cs-SPIONs)

1 g of chitosan biopolymer was dissolved in 100 mL of 1 % acetic acid solution and stirred for 5 h in a magnetic stirrer until a homogenous mixture was obtained. Then, 800 mg of finely powdered SPIONs was added to the above chitosan solution and kept for shaking in a rotary shaker for 18 h. This step is followed by ultrasonication for 30 min and centrifugation. After centrifugation, the supernatant was discarded and the pellet was washed to remove excess biopolymer solution. The resultant washed pellet was then lyophilized to obtain powder chitosan-coated SPIONs (Cs-SPIONs). The coated SPIONs were then utilized for further analysis and subjected to adsorption studies.

### Characterization Of SPIONs And Cs-SPIONs

The SPIONs and chitosan-coated SPIONs (Cs-SPIONs) were characterized using UV-visible spectroscopy (UV-1800, Shimadzu, Japan), FT-IR spectroscopy (IR affinity-1S, Shimadzu), scanning electron microscopy (SEM) (Carl Zeiss, Germany), energy-dispersive X-ray analysis (EDX), AFM microscopy (Bruker, Dimension icon model, Germany), XRD (Rigaku, Tokyo), zeta potential analysis (Brookhaven ZetaPALS, New York), vibrating sample magnetometer (VSM) with a maximum Magnetic field of 2.5 T and dynamic moment range of  $1 \times 10^{-6}$  emu– $10^3$  emu (Lakeshore, USA, Model 7407).

### Adsorption Studies

Adsorption study was performed to study the extent of removal of hexavalent chromium by SPIONs and chitosan-coated SPIONs (Cs-SPIONs).

### Adsorbate Preparation

For the study, different concentrations of chromium in parts per million (ppm) were prepared using potassium dichromate as the chromium salt. 0.14 g of potassium dichromate ( $K_2Cr_2O_7$ ) in 100 mL of MilliQ water corresponds to 500 ppm, and further dilution was done to obtain 100 ppm, 50 ppm, and 1 ppm of chromium solution. The prepared different concentrations of chromium solutions were tested against different dosages of adsorbents on different time intervals and pH in order to fix the optimal conditions.

### Chromium Detection Techniques

Two different methods were followed to detect the chromium in the treated supernatants by direct method and indirect or DPC method.

### Direct Method

Direct method is based on the UV-Vis absorbance maxima of chromium at 370 nm, usually performed for high concentration of chromium (above 1 ppm). In this method, the chromium in the treated supernatant was directly quantified by measuring their absorbance at 370 nm.

### Diphenyl carbazide (DPC) method or Indirect Method

Chromium concentration less than 1 ppm can be detected using DPC method. Here, 1 mL of the treated supernatant was added with 30  $\mu$ L of 2 N  $H_2SO_4$  to initiate  $Cr^{6+}$  dissociation followed by addition of 20  $\mu$ L of DPC (250 mg of DPC in 50 mL methanol/carbinol) to bind with  $Cr^{6+}$ . The interaction with DPC produced reddish-violet colour, which was spectrophotometrically analyzed at 540 nm.<sup>31,32</sup>

### Adsorbent Optimization

Different concentrations of each adsorbent, i.e., SPIONs and Cs-SPIONs, were taken in a range of 0.5 g/L to 7 g/L separately in order to determine the concentration which serves as a better adsorbent. These concentrations were added to different flasks containing 100 mL of 1 ppm chromium solution. They were left in the shaker to interact for 2 h and later indirect method of chromium determination was performed. The obtained OD values were taken in order to calculate the final concentration of chromium (using standard graph) and the percentage removal. A graph was plotted with concentration of adsorbent on X-axis and % removal on Y-axis.

$$\% \text{ removal} = \frac{\left( \frac{\text{Initial concentration} - \text{Final concentration}}{\text{Initial concentration}} \right) \times 100}{\text{Initial concentration}}$$

### Adsorbent–Adsorbate Concentration Optimization

In this stage, the best adsorbent (Cs-SPIONs) was used and evaluated for the optimal dosage of adsorbent concentration for chromium removal. Along with the adsorbent, chromium concentration was also optimized. Different concentrations of Cs-SPION 1g/L to 10 g/L were taken as a set. Each set of Cs-SPIONs was added to different flasks containing varied chromium concentrations like 1 ppm, 50 ppm, 100 ppm, and 500 ppm. It was then left for interaction for 2 h under constant rotation, and later, the supernatant was analysed for chromium concentration. From the OD values, the final concentration of chromium (using standard graph) and the percentage removal was calculated, and a graph was

plotted with the concentration of adsorbent on *X*-axis and % removal on *Y*-axis.

### Optimization Of Time Interval

In order to optimize the time required for the complete adsorption of chromium ions by Cs-SPIONs, the required dosages of Cs-SPIONs were taken and added to 50 ppm chromium concentration. The solution was stirred constantly and the supernatant from centrifugation was taken at 15 min interval for 2 h. The supernatant was analysed by the direct method. From the OD values, the final concentration of chromium (using standard graph) and the percentage removal were calculated and a graph was plotted with time interval on *X*-axis and % removal on *Y*-axis.

### pH Optimization

pH optimization was done to know the adsorption at different pH and to understand if acidic pH favours adsorption more. In this experiment, different pH ranging from 1 to 6 was maintained in different flasks containing 100 mL of 50 ppm chromium solution. The pH was set using 0.5 M NaOH and 4 N HNO<sub>3</sub>. Three sets of the above-mentioned pH ranges were taken. To each of these sets, Cs-SPIONs of 1 g/L, 5 g/L, and 10 g/L concentrations were added and allowed to interact for 2 h. Later, the supernatant was collected at the end of incubation and analyzed using the direct method. From the OD values, the final concentration of chromium (using standard graph) and the percentage removal were calculated, and a graph was plotted with pH on *X*-axis and % removal on *Y*-axis.

### Adsorption Isotherm

After optimization of all the parameters such as adsorbent–adsorbate concentrations, time, and pH, the data were used to plot isotherms for the study. Three isotherms, namely, Langmuir ( $1/q_e$  vs  $1/C_e$ ), Freundlich ( $\ln Q_e$  vs  $\ln C_e$ ), and Temkin ( $q_e$  vs  $\ln C_e$ ) isotherms, were plotted by calculating the  $C_e$ ,  $Q_e$ ,  $1/C_e$ ,  $\ln C_e$ ,  $1/Q_e$ , and  $\ln Q_e$  values.

$Q_e = (C_i - C_e) V/m$ ;  $C_i$  = initial concentration;  $C_e$  = final concentration;  $V$  = volume;  $m$  = mass.

### Adsorbent Characterization

After the adsorption studies were done, the pellet of adsorbed Cs-SPIONs obtained by centrifugation was dried. This adsorbent sample was subjected for analysing its magnetic properties after adsorption studies by vibrating sample magnetometer (VSM) (Lakeshore, USA, Model 7407).

## Results And Discussions

### Characterization Of SPIONs And Cs-SPIONs

#### UV-Visible Spectroscopy (UV-VIS)

UV-Vis spectroscopy showed the highest peak from 260 nm (Figure 1A) which confirmed the presence of iron oxide nanoparticles.<sup>18</sup> Chitosan-coated SPIONs (Cs-SPIONs) were analysed for the presence of chitosan biopolymer and iron oxide nanoparticles. The peaks formed at 392 nm and 260 nm (Figure 1B) confirmed the presence of chitosan and iron oxides, respectively.<sup>33</sup>

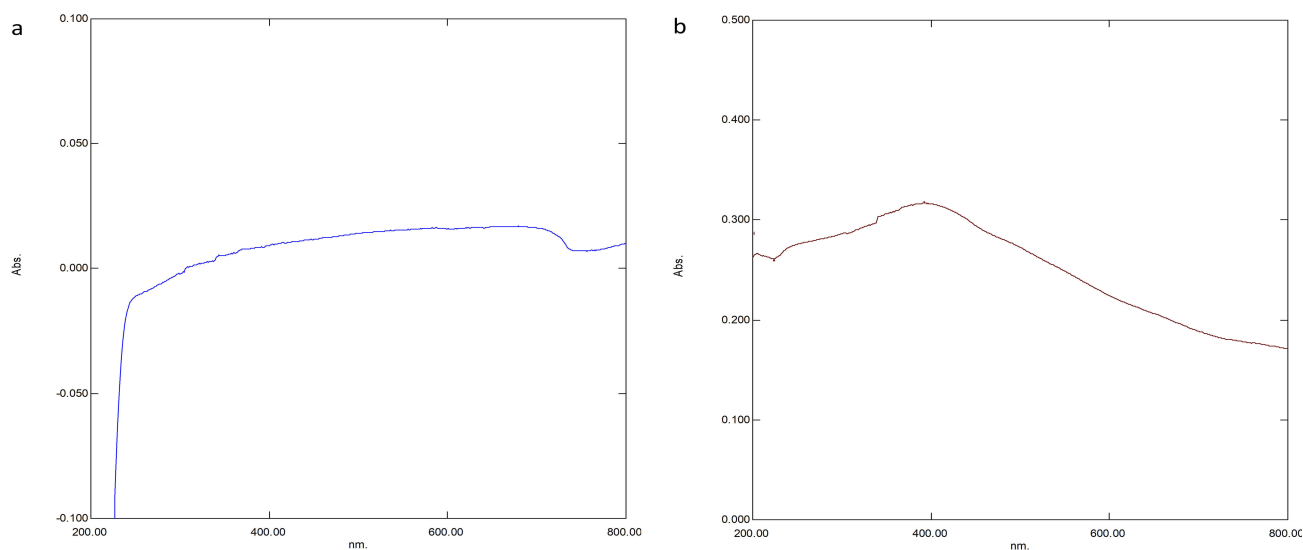


**Figure 1** UV - Vis analysis (A) SPIONs, (B) Cs-SPIONs.

### Fourier Transform-Infrared Spectroscopy (FT-IR)

FTIR analysis of SPIONs showed bands at  $3418.75\text{ cm}^{-1}$  and  $1596.19\text{ cm}^{-1}$  (Figure 2A) which corresponded to the stretching ( $\nu$ ) and bending ( $\delta$ ) vibrations, respectively. This was due to adsorbed water on the surface of the iron oxide nanoparticles. The band observed at  $584.65\text{ cm}^{-1}$  corresponded to the stretching vibrations of  $\text{Fe}_{(\text{tetrahedral})}\text{-O-Fe}_{(\text{octahedral})}$ . Thus, from the spectrum, it can be concluded the sample is iron oxide nanoparticles.<sup>34</sup> The FTIR results of Cs-SPIONs (Figure 2B) confirmed the biopolymer coating onto the SPIONs with peaks at  $2818.07\text{ cm}^{-1}$ ,  $1600.06\text{ cm}^{-1}$ ,  $1483.35\text{ cm}^{-1}$ , and  $1078.62\text{ cm}^{-1}$  corresponding to the stretching vibrations of  $\text{-CH}$ ,  $\text{N-H}$ ,  $\text{C-N}$  vibration of amino group and  $\text{C-O}$  in the ether group of chitosan, respectively.<sup>33</sup>

### Scanning Electron Microscopy (SEM)

The surface morphology and size of the nanoparticles were found out using scanning electron microscope. The images obtained from SEM analysis showed that the average particle size of synthesized SPIONs was ranging around 9–25 nm (Figure 3A), with the smallest particles having the size of around 9–10 nm and the largest particles having a size around 22–25 nm.<sup>34</sup> SEM imaging also revealed the surface morphology and size of the SPIONs after coating with chitosan (Cs-SPIONs) having an average particle size ranging around 30–40 nm (Figure 3B).

### Energy-Dispersive X-Ray (EDAX)

In this analysis, the synthesized SPIONs were detected with the elements Fe and O (Figure 4A), thus confirming the presence of iron oxides. EDAX analysis of Cs-SPIONs showed the presence of the major elements such as C, O, and Fe which was the representation of iron oxides and chitosan biopolymer (Figure 4B).

### Atomic Force Microscopy (AFM)

The three-dimensional structure of the SPIONs was seen using atomic force microscope. Here, the particles were found to be around 20 nm with cubical shape (Figure 5A). Chitosan-coated nanoparticles were found to be around 28–41 nm with cubical shape (Figure 5B).

### X-Ray Diffraction Spectroscopy (XRD)

XRD pattern showed that the particles were highly crystalline with high intensity peaks at  $32.01^\circ$  (220),  $35.67^\circ$  (311),  $43.17^\circ$  (400),  $54.03^\circ$  (422),  $56.79^\circ$  (511), and  $62.76^\circ$  (440) (Figure 6A) which were in accordance with the values of  $\text{Fe}_3\text{O}_4$  XRD graph of JCPDS data number 87–2334.<sup>35</sup> Hence, the particles were confirmed to be magnetite nanoparticles. XRD analysis of Cs-SPIONs showed the particles to be highly crystalline in nature with sharp peaks at  $10.44^\circ$ , which is a characteristic peak for chitosan (Figure 6B). The rest of the peaks were in par with the peaks of  $\text{Fe}_3\text{O}_4$  with high-intensity peaks at (220), (311), (400), (422), (511), and (440).<sup>36</sup>



**Figure 2** FT-IR analysis (A) SPIONs, (B) Cs-SPIONs.

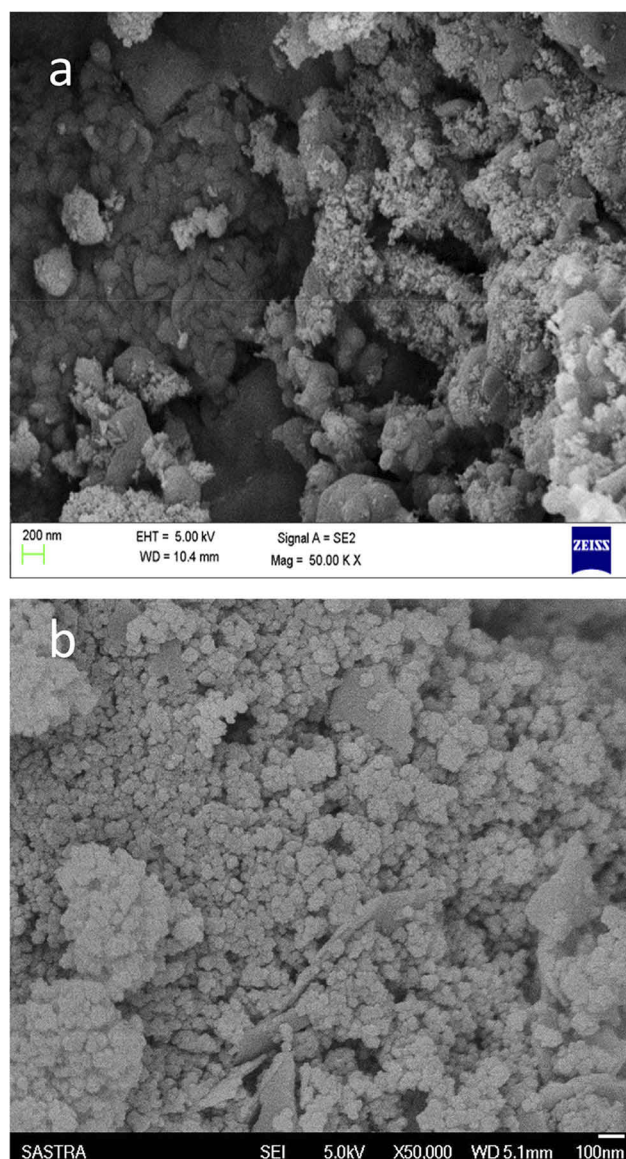


**Figure 3** SEM vis analysis (A) SPIONs, (B) Cs-SPIONs.

### Zeta Potential Analysis

SPIONs were seen to have a charge of  $-13.43$  mV (Figure 7A). Any value above  $+25$ mV and below  $-25$ mV is said to be stable in nature.<sup>37</sup> SPIONs were found to be unstable and needed surface functionalization or engineering to make them stable and less aggregated that would be favourable for further studies. Cs-SPIONs were seen to have a charge of  $-25.51$  mV (Figure 7B) and found to be stable.

### Vibrating Sample Magnetometer (VSM)

The M-H hysteresis curve of the SPIONs showed to have a slight hysteresis curve with magnetization around  $84.901$  emu/g (Figure 8A and B). Both SPIONs and Cs-SPIONs

were found to be super-paramagnetic in nature with slightly ferromagnetic features.<sup>38</sup>

## Adsorption Studies

### Adsorbent Optimization

This experiment was performed in order to determine the best adsorbent between SPIONs and Cs-SPIONs. Different dosages of these adsorbents were taken and checked for the removal of  $1$  ppm  $\text{Cr}^{6+}$  heavy metal ions from the solution. It was seen that at  $7$  g/L dosage of adsorbent,  $80.44\%$  and  $99.7\%$  removal was attained by SPIONs and Cs-SPIONs, respectively (Figure 9). Hence, this proved that Cs-SPIONs were better adsorbents than

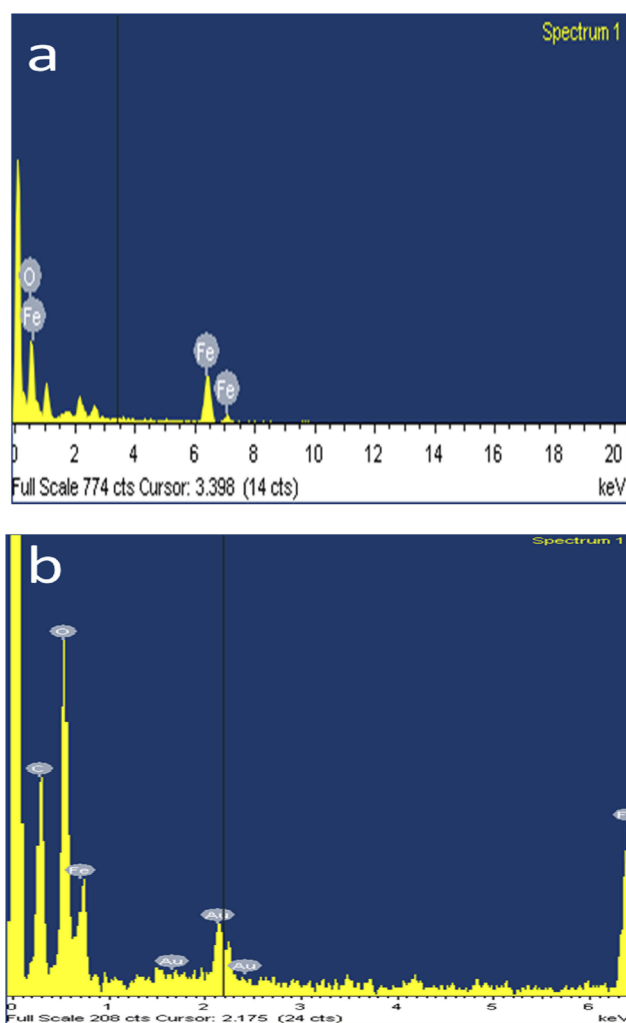


**Figure 4** EDX analysis (A) SPIONs, (B) Cs-SPIONs.

naked SPIONs, and so Cs-SPIONs were utilized for further studies. Chitosan is a cationic polysaccharide molecule whose amine group may be involved in coating against the synthesised negatively charged SPIONs, whereas for the chromium adsorption, it is predicted that the redox reaction in hydroxyl group of chitosan as well as the negative charge of SPIONs can support for an ionic interaction towards chromium ions ( $\text{Cr}^{+}$ ). When bis (2,4,4-trimethylpentyl)-dithiophosphinic acid (Cyanex-301)-coated SPIONs were checked for chromium removal, it was proposed that the complexation between the thiol group on Cyanex-301 and Cr (VI) ions promoted the chromium adsorption.<sup>39</sup> Polymer-coated iron oxide (polyMETAC-2(methacryloyloxy)ethyl trimethyl-ammonium chloride) were produced by Hanif and Shahzad<sup>40</sup> to treat contaminated water containing chromium ions Cr (VI) and dye (alizarin). This polycationic polymer-based iron oxides have also resulted in removal by 80–96% of

dye and 62–91% of chromium Cr(VI). To be more analogous with the above-reported results with Cs-SPIONs, the chitosan–magnetite nanocomposite strip was developed by Sureshkumar et al<sup>41</sup> where they showed similar adsorption efficiency. These strips were checked for chromium adsorption, where chitosan–magnetite nanocomposite strips exhibited better chromium ion removal (92.33%) when compared with chitosan strips (29.39%). Thus, it is very obvious that iron oxide nanoparticles can be used as a potent water remediation tool via different surface fabrication.

#### Adsorbent–Adsorbate Concentration Optimization

Optimization of the concentrations of adsorbent (Cs-SPIONs) and adsorbate (hexavalent chromium) was done by taking various concentrations of nanoparticles and chromium solutions. The extend of proficiency of adsorption in each set was recorded and analysed. Through this

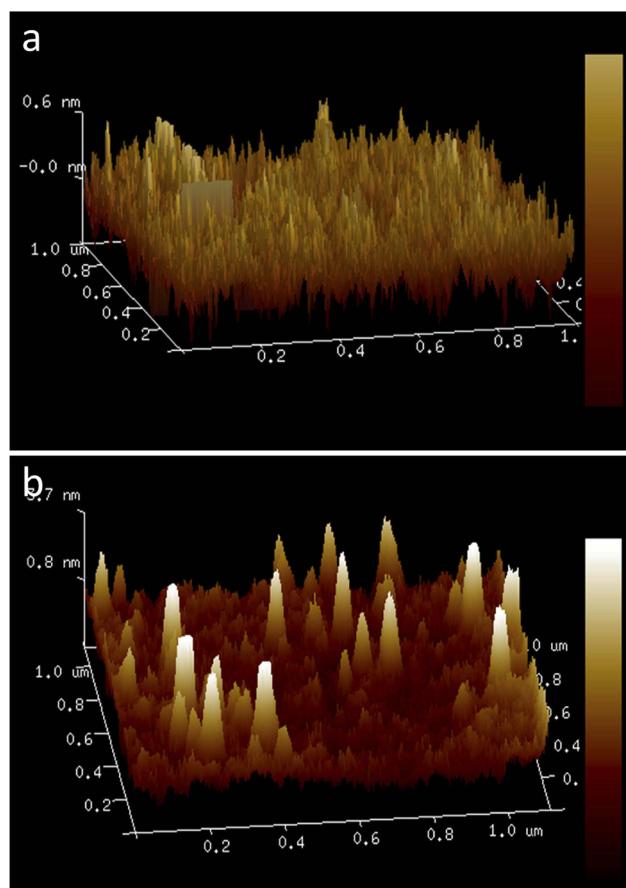


**Figure 5** AFM analysis (A) SPIONs, (B) Cs-SPIONs.

study, it was found that the highest concentration of Cs-SPIONs, i.e., 10 g/L, was observed to have the highest adsorption efficiency in all the chromium concentrations except 500 ppm. The maximum removal of 98.2% by 10 g/L was seen in 50 ppm of chromium solution (Figure 10). Hence, the concentrations were optimized to be 10 g/L for Cs-SPIONs and 50 ppm for chromium ions. Having a

similar study design of optimization, the removal of nickel heavy metal ions from industrial effluents was examined in a bioreactor using chitosan-coated magnetic nanoparticles as the adsorbent.<sup>42</sup> The optimal conditions for efficient nickel ion removal were reached at retention time (20–60 mins) with the adsorbent concentration at 0.09–1 g/L and pH level (0.5–9). Maximum removal rates to 83% and

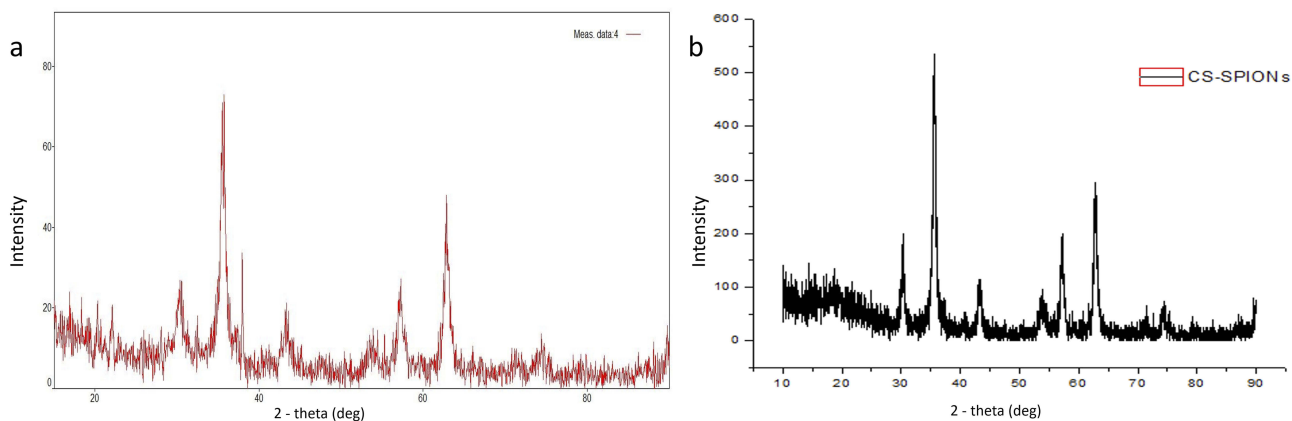


**Figure 6** XRD analysis (A) SPIONs, (B) Cs-SPIONs.



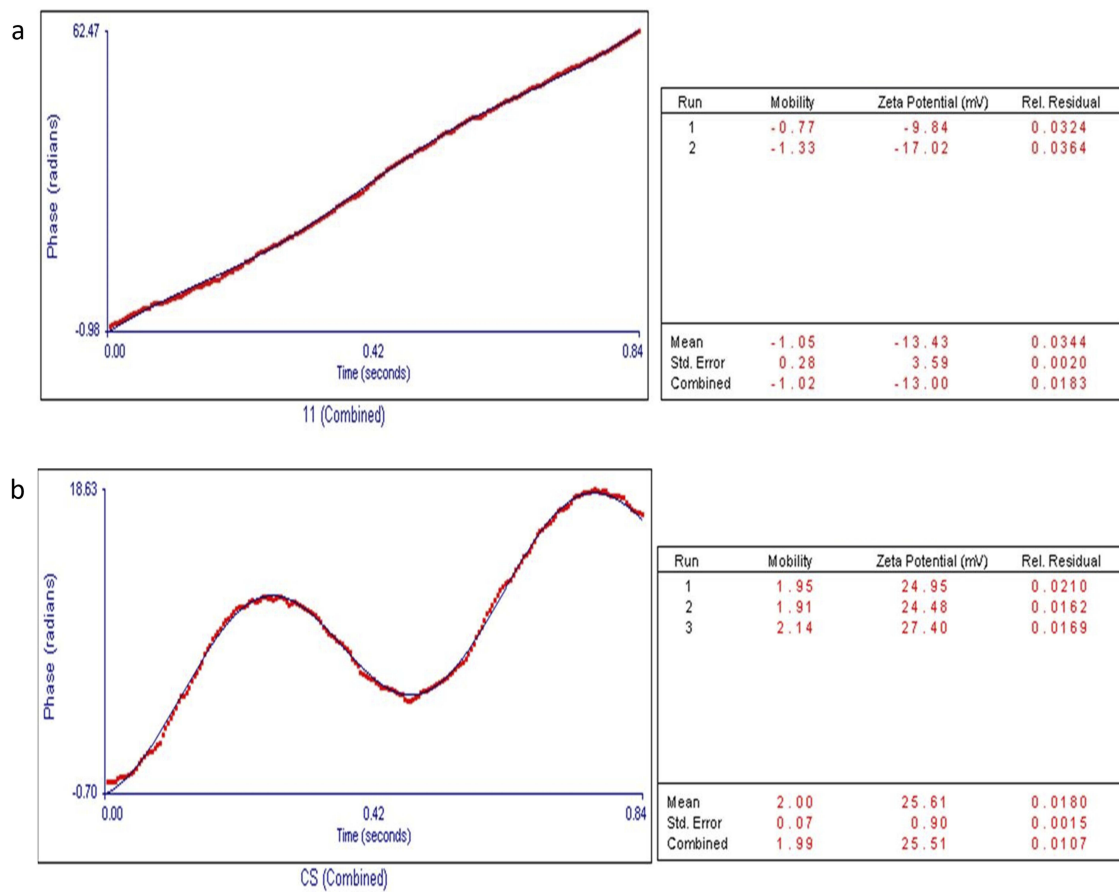


Figure 7 Zeta potential analysis (A) SPIONs (B) Cs-SPIONs.

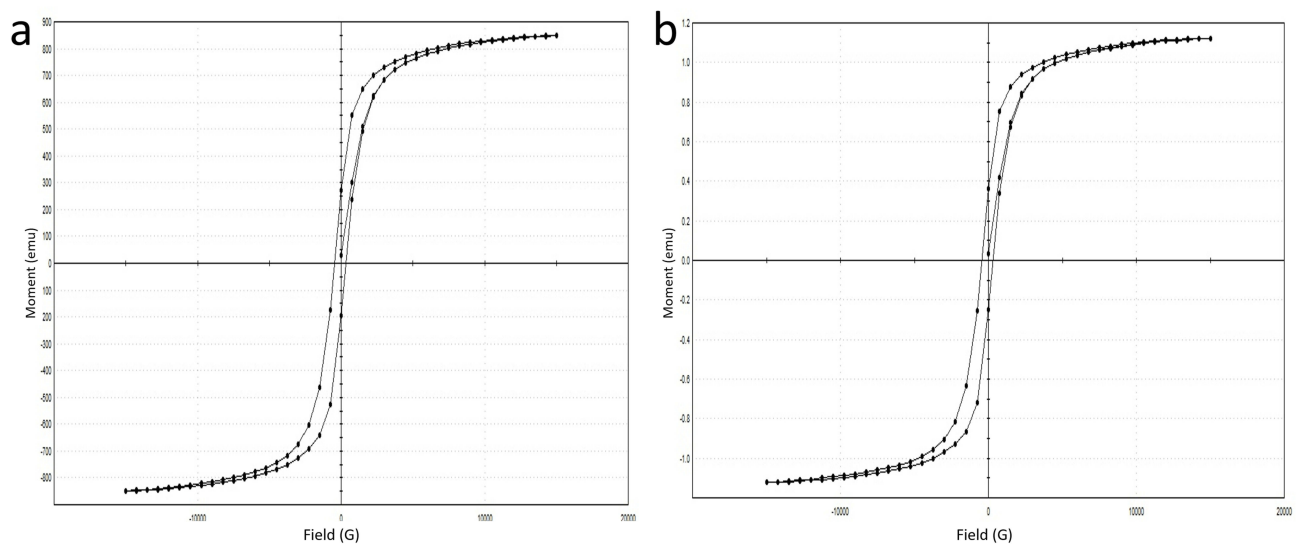


Figure 8 VSM analysis (A) SPIONs, (B) Cs-SPIONs.

92.1% were accomplished for nickel heavy metal ions from synthetic and industrial effluents using chitosan-coated magnetic nanoparticle.<sup>42</sup>

### Optimization Of Time Interval

In order to determine the optimum time period where maximum efficiency is reached, different dosages of Cs-SPIONs

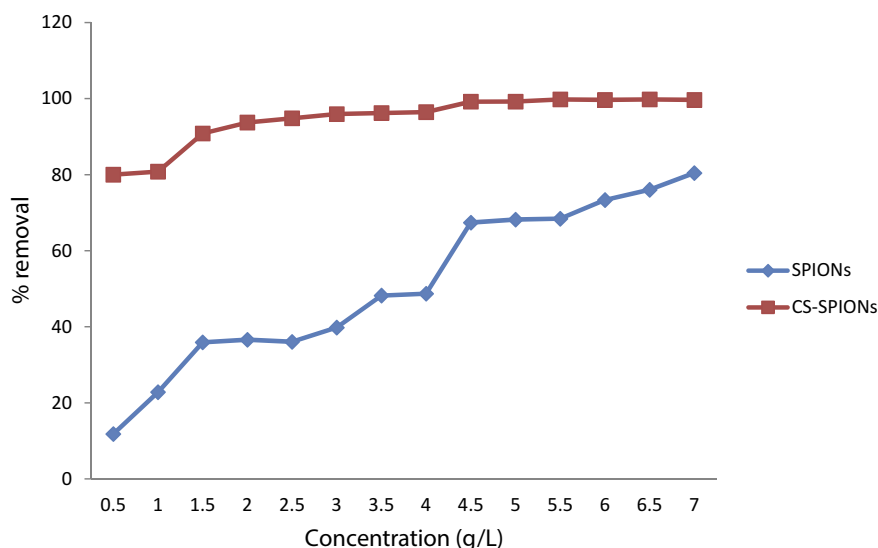


Figure 9 Adsorbent optimization for chromium removal.

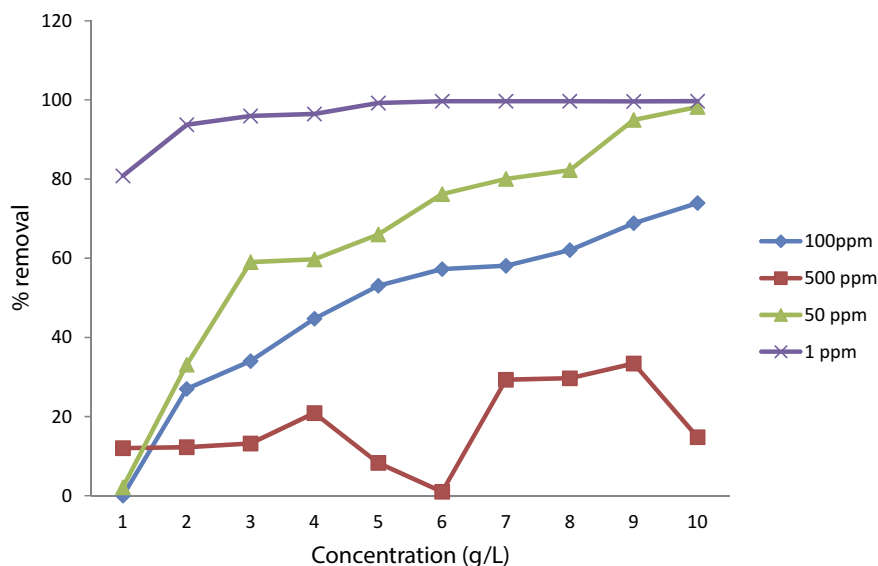


Figure 10 Optimization of adsorbent-adsorbate concentration.

were taken in 50 ppm chromium solution and checked for % removal at every 15 min for 2 h. Maximum removal was seen at 105<sup>th</sup> min for 3 g/L, 5 g/L, and 10 g/L and at 120<sup>th</sup> min for 7 g/L and 9 g/L (Figure 11).

**pH Optimization**

pH optimization was done to check the effect of pH in the adsorption rate. Hence, different concentrations of Cs-SPIONs in 50 ppm chromium solution were taken to understand the difference in % removal with respect to pH change. The change in the removal at two different time intervals was

also checked to understand the pH effect in a better way. It was seen that as the pH decreases, the removal efficiency has steadily increased and the maximum efficiency was seen at pH 2 (Figure 12). The % removal was also greater at 60<sup>th</sup> and 120<sup>th</sup> min at pH 2 when compared to other pH ranges. This showed that removal efficiency and adsorption were greatly influenced by pH and must be because of hexavalent Cr ion conversion into trivalent which are relatively easier to be removed. More comparable pH effect for chromium removal was conveyed by Bhaumik et al<sup>43</sup> using Fe<sub>3</sub>O<sub>4</sub>-coated polypyrrole magnetic composite where 100% adsorption of Cr(VI)

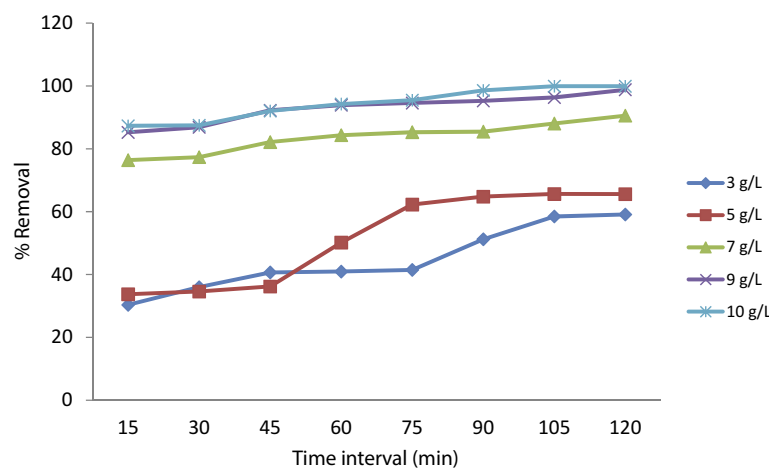


Figure 11 Optimization of time period for chromium removal.

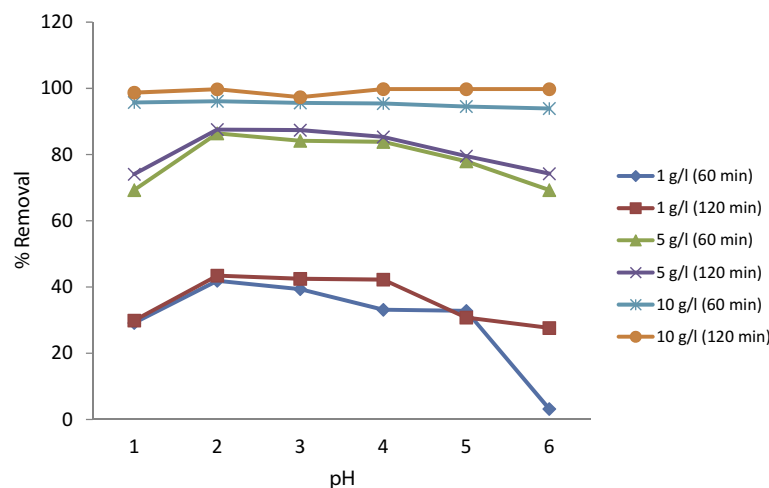


Figure 12 Optimization of pH for chromium removal.

was attained at pH 2. The adsorption efficiency was greater at lower pH and concluded that ionic exchange or reduction at the adsorbent could possibly be the driving force for Cr(VI) removal. The better response of Cs-SPIONs against chromium removal at low pH can be understood by analysing the facts of surface chemistry at the aqueous phase. Metal oxides are generally covered by hydroxyl group, which tends to vary in its form at different pH. For iron oxides, the surface charge becomes neutral at pH 5.8, further lowering the pH will render the adsorbent surface rich of hydronium ions which acts as positively charged surface. Also that Cr(VI) species predominantly exists as monovalent bichromate ( $\text{HCrO}_4^-$ ) and divalent dichromate ( $\text{Cr}_2\text{O}_7^{2-}$ ) at lower pH. This creates electrostatic attraction between the hydronium ions and chromium ions

resulting in better adsorption. However, chromium ions also compete for the protons at the lower pH.<sup>44,45</sup>

### Adsorption Isotherm

With the given data of adsorption, three different adsorption isotherms are plotted, namely, Langmuir isotherm, Freundlich isotherm, and Temkin isotherm. From the isotherm data (Figure 13), it is observed that the  $R^2$  value of Freundlich isotherm is 0.928 which implies that the given adsorbent and the nature of adsorption happening are in relevance with Freundlich isotherm. From this, it can be stated that the nature of adsorption is multilayered and homogenous with non-uniform distribution. Similar experimentation was performed by Samrot et al<sup>33</sup> using chitosan-coated SPIONs and subjected to chromium removal studies. These

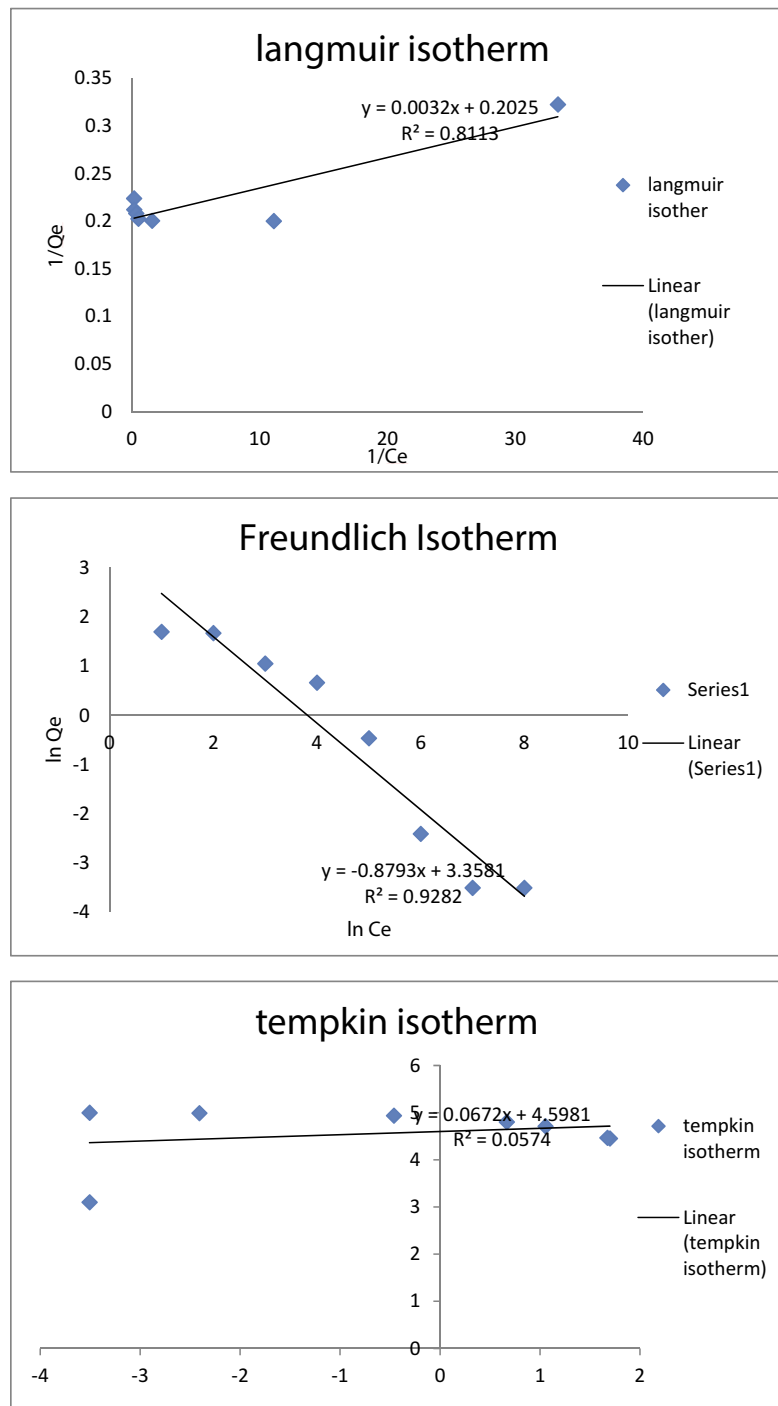


**Figure 13** Isotherm studies for chromium removal.

chitosan-coated SPIONs were found to show 80% of chromium removal efficiency and the adsorption mechanism was the same as that of the above-reported isotherm, i.e., Freundlich isotherm whose adsorption efficacy was dependent on the concentration of adsorbent and adsorbate used.

Jiang et al<sup>46</sup> produced magnetically separable millimeter-sized chitosan beads containing nanosized  $\gamma\text{-Fe}_2\text{O}_3$  and used these beads for chromium removal. The adsorption pattern of chromium ions onto  $\gamma\text{-Fe}_2\text{O}_3$ -loaded chitosan beads was corresponding to Freundlich isotherm as well.

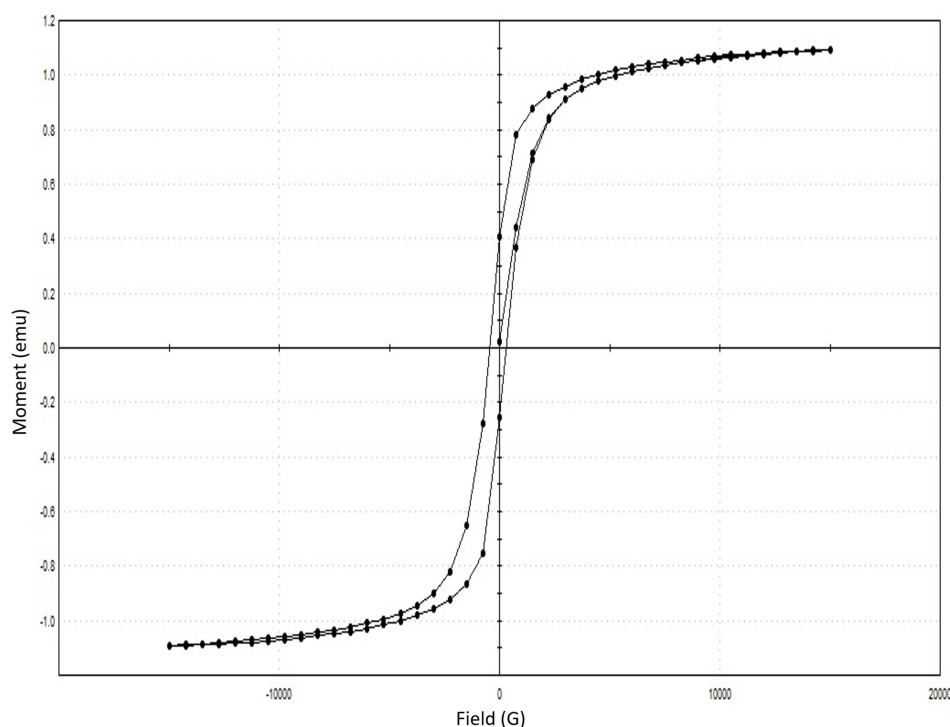


**Figure 14** Vibrating sample magnetometer of Cs-SPIONs after adsorption.

### Adsorbent Characterization

VSM analysis of Cs-SPIONs after adsorption (Figure 14) also showed that the magnetization has not changed throughout the adsorption process. The particles were seen to be superparamagnetic with slight ferromagnetic qualities.<sup>38</sup>

### Conclusion

From this study, it can be concluded that chitosan-coated SPIONs (Cs-SPIONs) can have a cumulative effect in removing heavy metals such as hexavalent chromium efficiently. It was also found that the removal efficiency is maximum at acidic pH, i.e., at a pH of 2, and 10 g/L adsorbents can efficiently remove up to 50 ppm of hexavalent chromium ions. From this study, it can be said that Cs-SPIONs can be efficiently used in treating and removing chromium heavy metal ions from groundwaters in a proper controlled treatment system.

### Disclosure

The authors report no conflicts of interest in this work.

### References

1. Tchounwou PB, Yedjou CG, Patlolla AK, Sutton DJ. Heavy metal toxicity and the environment. *Exp Suppl.* 2012;101:133–164. doi:10.1007/978-3-7643-8340-4\_6

2. Järup L. Hazards of heavy metal contamination. *Br Med Bull.* 2003;68:167–182. doi:10.1093/bmb/ldg032
3. Owlad M, Aroua MK, Daud WAW, Baroutian S. Removal of hexavalent chromium-contaminated water and wastewater: a review. *Water Air Soil Pollut.* 2009;200(1):59–77. doi:10.1007/s11270-008-9893-7
4. Barnowski C, Jakubowski N, Stuewer D, Broekaert JAC. Speciation of chromium by direct coupling of ion exchange chromatography with ICP-MS. *At Spectrom.* 1997;1155(10):1155–1161. doi:10.1039/a702120h
5. Gil RA, Cerutti S, Gásquez JA, Olsina RA, Martínez LD. Preconcentration and speciation of chromium in drinking water samples by coupling of on-line sorption on activated carbon to ETAAS determination. *Talanta.* 2006;68(4):1065–1070. doi:10.1016/j.talanta.2005.06.069
6. Katz SA, Slem H. *The Biological and Environmental Chemistry of Chromium.* New York: VCH; 1994.
7. Kotas J, Stasicka Z. Chromium occurrence in the environment and methods of its speciation. *Environ Pollut.* 2000;107(3):263–283. doi:10.1016/s0269-7491(99)00168-2
8. Mohanraj VJ, Chen Y. Nanoparticles-a review. *Trop J Pharm Res.* 2006;5(1):561–573.
9. Erbil HY. *Surface Chemistry of Solid and Liquid Interfaces.* 1st ed. Oxford: Blackwell Publishing; 2006.
10. Wu JH, Shao FQ, Han SY, et al. Shape-controlled synthesis of well-dispersed platinum nanocubes supported on graphitic carbon nitride as advanced visible-light-driven catalyst for efficient photoreduction of hexavalent chromium. *J Colloid Interface Sci.* 2019;1(535):41–49. doi:10.1016/j.jcis.2018.09.080
11. Shao FQ, Feng JJ, Lin XX, Jiang LY, Wang AJ. Simple fabrication of AuPd@Pd core-shell nanocrystals for effective catalytic reduction of hexavalent chromium. *Appl Catalysis B.* 2017;208:128–134. doi:10.1016/j.apcatb.2017.02.051
12. Wu JH, Shao FQ, Luo XQ, Xu HJ, Wang AJ. Pd nanocones supported on g-C<sub>3</sub>N<sub>4</sub>: an efficient photocatalyst for boosting catalytic reduction of hexavalent chromium under visible-light irradiation. *Appl Surf Sci.* 2019;471:935–942. doi:10.1016/j.apsusc.2018.12.075

13. Li DN, Shao FQ, Feng JJ, Wei J, Zhang QL, Wang AJ. Uniform Pt@Pd nanocrystals supported on N-doped reduced graphene oxide as catalysts for effective reduction of highly toxic chromium(VI). *Mater Chem Phys*. 2018;205:64–71. doi:10.1016/j.matchemphys.2017.10.074
14. Hu LY, Chen LX, Liu MT, Wang AJ, Wu LJ, Feng JJ. Theophylline-assisted, eco-friendly synthesis of PtAu nanospheres at reduced graphene oxide with enhanced catalytic activity towards Cr(VI) reduction. *J Colloid Interface Sci*. 2017;493:94–102. doi:10.1016/j.jcis.2016.12.068
15. Saini R, Saini S, Sharma S. Nanotechnology: the future medicine. *J Cutan Aesthet Surg*. 2010;3(1):32–33. doi:10.4103/0974-2077.63301
16. Khan I, Saeed K, Khan I. Nanoparticles: properties, applications and toxicities. *Arabian J Chem*. 2017. doi:10.1016/j.arabjc.2017.05.011
17. Goya GF, Berquo TS, Fonseca FC, Morales MP. Static and dynamic magnetic properties of spherical magnetite nanoparticles. *J Appl Phys*. 2003;94(5):3520–3528. doi:10.1063/1.1599959
18. Justin C, Philip SA, Samrot AV. Synthesis and characterization of superparamagnetic iron-oxide nanoparticles (SPIONs) and utilization of SPIONs in X-ray imaging. *Appl Nanosci*. 2017;7(7):463–475. doi:10.1007/s13204-017-0583-x
19. Gupta AK, Gupta M. Synthesis and surface engineering of iron oxide nanoparticles for biomedical applications. *Biomaterials*. 2005;26(18):3995–4021. doi:10.1016/j.biomaterials.2004.10.012
20. Shubayev VI, Pisanic TR II, Jin S. Magnetic nanoparticles for theragnostics. *Adv Drug Deliv Rev*. 2009;61(6):467–477. doi:10.1016/j.addr.2009.03.007
21. Sethi M, Chakarvarti SK. Hyperthermia Techniques for cancer treatment: a Review. *Int J Pharmtech Res*. 2015;8(6):292–299.
22. Kalber TL, Ordidge KL, Southern P, et al. Hyperthermia treatment of tumors by mesenchymal stem cell-delivered superparamagnetic iron oxide nanoparticles. *Int J Nanomedicine*. 2016;11:1973–1983. doi:10.2147/IJN.S94255
23. Lee H, Yu MK, Park S, et al. Thermally cross-linked superparamagnetic iron oxide nanoparticles: synthesis and application as a dual imaging probe for cancer in vivo. *J Am Chem Soc*. 2007;129(42):12739–12745. doi:10.1021/ja072210i
24. Justin C, Samrot AV, Sahithya CS, Bhavya KS, Saipriya C. Preparation, characterization and utilization of coreshell superparamagnetic iron oxide nanoparticles for curcumin delivery. *PLoS One*. 2018;13(7):1–18. doi:10.1371/journal.pone.0200440
25. Heidari F, Bahrololoom ME, Vashae D, Tayebi L. In situ preparation of iron oxide nanoparticles in natural hydroxyapatite/chitosan matrix for bone tissue engineering application. *Ceramics Int*. 2015;41(2):3094–3100. doi:10.1016/j.ceramint.2014.10.153
26. Babic M, Horák D, Trchová M, et al. Poly (L-lysine)-modified iron oxide nanoparticles for stem cell labelling. *Bioconjugate Chem*. 2008;19(3):740–750. doi:10.1021/bc700410z
27. Samrot AV, Senthilkumar P, Rashmitha S, Veera P, Sahithya CS. Azadirachta indica influenced biosynthesis of super-paramagnetic iron-oxide nanoparticles and their applications in tannery water treatment and X-ray imaging. *J Nanostructure Chem*. 2018;8(3):343–351. doi:10.1007/s40097-018-0279-0
28. No HK, Meyers SP. Application of chitosan for treatment of wastewaters. *Rev Environ Contam Toxicol*. 2000;163:1–27.
29. Guibal E. Interactions of metal ions with chitosan-based sorbents: a review. *Sep Purif Technol*. 2004;38(1):43–74. doi:10.1016/j.seppur.2003.10.004
30. Rojas G, Silva J, Flores JA, Rodriguez A, Ly M, Maldonado H. Adsorption of chromium onto cross-linked chitosan. *Sep Purif Technol*. 2005;44(1):31–36. doi:10.1016/j.seppur.2004.11.013
31. Stover NM. Diphenylcarbazide as a test for chromium. *J Am Chem Soc*. 1928;50(9):2363–2366. doi:10.1021/ja01396a007
32. Shigematsu T, Gohda S, Yamazaki H, Nishikawa Y. Spectrophotometric determination of Chromium (III) and Chromium (VI) in sea water. *Bull Inst Chem Res*. 1978;55(5):429–440.
33. Samrot AV, Shobana N, Sruthi PD, Sahithya CS. Utilization of chitosan-coated superparamagnetic iron oxide nanoparticles for chromium removal. *Appl Water Sci*. 2018;8(7):192. doi:10.1007/s13201-018-0841-4
34. Kayal S, Ramanujan RV. Doxorubicin loaded PVA coated iron oxide nanoparticles for targeted drug delivery. *Mater Sci Eng C Mater Biol Appl*. 2010;30(3):484–490. doi:10.1016/j.msec.2010.01.006
35. Balasubramanian C, Joseph B, Gupta P, et al. X-ray absorption spectroscopy characterization of iron-oxide nanoparticles synthesized by high temperature plasma processing. *J Electron Spectrosc Relat Phenomena*. 2014;196:125–129. doi:10.1016/j.elspec.2014.02.011
36. Kumar S, Koh J. Physicochemical, optical and biological activity of chitosan-chromone derivative for biomedical applications. *Int J Mol Sci*. 2012;13(5):6102–6116. doi:10.3390/ijms13056102
37. Greenwood R, Kendall K. Selection of suitable dispersants for aqueous suspensions of zirconia and titania powders using acoustophoresis. *J Eur Ceram Soc*. 1999;19(4):479–488. doi:10.1016/S0955-2219(98)00208-8
38. Mahmoudi M, Simchi A, Imani M, et al. A new approach for the in vitro identification of the cytotoxicity of superparamagnetic iron oxide nanoparticles. *Colloids Surf B Biointerfaces*. 2010;75(1):300–309. doi:10.1016/j.colsurfb.2009.08.044
39. Burks T, Uheida A, Saleemi M, Eita M, Toprak MS, Muhammed M. Removal of Chromium (VI) using surface modified superparamagnetic iron oxide nanoparticles. *Sep Sci Technol*. 2013;48(8):1243–1251. doi:10.1080/01496395.2012.734364
40. Hanif S, Shahzad A. Removal of chromium(VI) and dye Alizarin Red S (ARS) using polymer-coated iron oxide (Fe<sub>3</sub>O<sub>4</sub>) magnetic nanoparticles by co-precipitation method. *J Nanopart Res*. 2013;16:2429. doi:10.1007/s11051-014-2429-8
41. Sureshkumar V, Daniel KSCG, Ruckmani K, Sivakumar M. Fabrication of chitosan-magnetite nanocomposite strip for chromium removal. *Appl Nanosci*. 2016;6:277. doi:10.1007/s13204-015-0429-3
42. Esmaeili A, Farrahi NT. The efficiency of a novel bioreactor employing bacteria and chitosan-coated magnetic nanoparticles. *J Taiwan Inst Chem Eng*. 2016;59:113–119. doi:10.1016/j.jtice.2015.08.022
43. Bhaumik M, Maity A, Srinivasu VV, Onyango MS. Enhanced removal of Cr(VI) from aqueous solution using polypyrrole/Fe<sub>3</sub>O<sub>4</sub> magnetic nanocomposite. *J Hazard Mater*. 2011;190(1–3):381–390. doi:10.1016/j.jhazmat.2011.03.062
44. Shalaby TI, Fikrt NM, Mohamed MM, El Kady MF. Preparation and characterization of iron oxide nanoparticles coated with chitosan for removal of Cd(II) and Cr(VI) from aqueous solution. *Water Sci Technol*. 2014;70(6):1004–1010. doi:10.2166/wst.2014.315
45. Zhang S, Zhou Y, Nie W, Song L, Zhang T. Preparation of uniform magnetic chitosan microcapsules and their application in adsorbing copper ion(II) and chromium ion(III). *Ind Eng Chem Res*. 2012;51(43):14099–14106. doi:10.1021/ie301942j
46. Jiang YJ, Yu XY, Luo T, Jia Y, Liu JH, Huang XJ.  $\gamma$ -Fe<sub>2</sub>O<sub>3</sub> nanoparticles encapsulated millimeter-sized magnetic chitosan beads for removal of Cr (VI) from water: thermodynamics, kinetics, regeneration, and uptake mechanisms. *J Chem Eng Data*. 2013;58(11):3142–3149. doi:10.1021/je400603p

## International Journal of Nanomedicine

Dovepress

### Publish your work in this journal

The International Journal of Nanomedicine is an international, peer-reviewed journal focusing on the application of nanotechnology in diagnostics, therapeutics, and drug delivery systems throughout the biomedical field. This journal is indexed on PubMed Central, MedLine, CAS, SciSearch<sup>®</sup>, Current Contents<sup>®</sup>/Clinical Medicine,

Journal Citation Reports/Science Edition, EMBase, Scopus and the Elsevier Bibliographic databases. The manuscript management system is completely online and includes a very quick and fair peer-review system, which is all easy to use. Visit <http://www.dovepress.com/testimonials.php> to read real quotes from published authors.

Submit your manuscript here: <https://www.dovepress.com/international-journal-of-nanomedicine-journal>